

NJC

New Journal of Chemistry

A journal for new directions in chemistry

Accepted Manuscript

This article can be cited before page numbers have been issued, to do this please use: Y. Bai, M. Wu, Q. Ma, C. Wang, J. Sun, M. Tian and J. Li, *New J. Chem.*, 2019, DOI: 10.1039/C9NJ03375K.



This is an Accepted Manuscript, which has been through the Royal Society of Chemistry peer review process and has been accepted for publication.

Accepted Manuscripts are published online shortly after acceptance, before technical editing, formatting and proof reading. Using this free service, authors can make their results available to the community, in citable form, before we publish the edited article. We will replace this Accepted Manuscript with the edited and formatted Advance Article as soon as it is available.

You can find more information about Accepted Manuscripts in the [Information for Authors](#).

Please note that technical editing may introduce minor changes to the text and/or graphics, which may alter content. The journal's standard [Terms & Conditions](#) and the [Ethical guidelines](#) still apply. In no event shall the Royal Society of Chemistry be held responsible for any errors or omissions in this Accepted Manuscript or any consequences arising from the use of any information it contains.

A FRET-based ratiometric fluorescent probe for highly selective detection of cysteine based on a coumarin-rhodol derivative

Yu Bai^a, Ming-Xia Wu^a, Qiu-Juan Ma^{a,*}, Chun-Yan Wang^a, Jing-Guo Sun^a, Mei-Ju Tian^a, Jian-Sheng Li^{b,*}

^a School of Pharmacy, Henan University of Chinese Medicine, Zhengzhou 450046, PR China

^b Collaborative Innovation Center for Respiratory Disease Diagnosis and Treatment & Chinese Medicine Development of Henan Province, Henan University of Chinese Medicine, Zhengzhou 450046, PR China

*Corresponding author, E-mail: maqiujuan104@126.com (Q. J. Ma); li_js8@163.com (J. S. Li);

Tel: +86-371-65676656; Fax: +86-371-65680028.

Abstract

Cysteine, as an important amino acid in the human body, plays a vital role in people's normal life activities. In this paper, a ratiometric fluorescent probe for detecting cysteine was designed and synthesized based on the fluorescence resonance energy transfer (FRET) process. In this FRET system, a coumarin derivative was used as the energy donor and a rhodol fluorophore was chosen as the energy receptor which was modified with an acrylate group as a cysteine recognition unit. In the absence of cysteine, the rhodol receptor was in the non-fluorescent lactone state and FRET process was inhibited. Upon addition of cysteine, the closed spirolactone form was converted to a conjugated fluorescent xanthenes form to induce the occurrence of FRET which resulted in a fluorescent signal decrease at 470 nm and enhancement at 543 nm. The ratiometric fluorescent probe exhibited excellent selectivity to Cys over Hcy and GSH. In addition, $I_{543\text{ nm}}/I_{470\text{ nm}}$ of the probe for cysteine displayed a good linear relationship in the range of 5.0×10^{-7} – 1.0×10^{-4} mol L⁻¹, and the detection limit was 2.0×10^{-7} mol L⁻¹. Furthermore, the probe showed low cell toxicity and had been successfully applied to the confocal imaging of cysteine in HepG2 cells by dual emission channels.

Keywords: ratiometric fluorescent probe; cysteine; FRET; coumarin-rhodol; cell imaging

1. Introduction

Cysteine is an important biothiol, a common amino acid in the body, which plays an important role in reversible redox reactions, cell detoxification and metabolism.^{1,2} The high or low content of the product may cause adverse reactions in the organism. For example, the loss of cysteine leads to reduced hematopoiesis, hair pigmentation, skin development damage and cancer.³⁻⁶ Increased cysteine levels can cause severe neurotoxicity and cardiovascular disease.⁷⁻⁹ Therefore, the development of efficient and reliable methods for the detection of cysteine is of great significance for the early diagnosis and treatment of diseases.

The methods for detecting cysteine in recent years include high-performance liquid chromatography (HPLC),^{10,11} capillary electrophoresis (CE),^{12,13} ultraviolet-visible spectroscopic spectroscopy (UV-Vis),¹⁴ and Fourier transform infrared (FTIR) spectrophotometry,¹⁵ fluorescence spectroscopy.^{16,17} Among them, the fluorescent probe has the advantages of high sensitivity, good selectivity, easy manipulation, no damage to the test sample, and can be combined with fluorescence imaging technology for the in situ detection of Cys in living cells, tissues and organisms. Real-time imaging and monitoring of related biological processes have become an effective and reliable means of detection.¹⁸⁻²² Fluorescent probes currently used for cysteine often utilize nucleophilicity of thiol group or high transition metal affinity of thiol group. The detection mechanisms involve Michael addition reaction,^{23,24} Michael addition and intramolecular cyclization reaction,²⁵⁻²⁸ cyclization with aldehyde,^{29,30} cleavage of sulfonamide and sulfonate ester,^{31,32} cleavage of disulfide,³³ cleavage of Se-N bond,³⁴ meal complexes-displace coordination^{35,36} and others³⁷⁻³⁹. Nevertheless, most of the reported fluorescent probes are used to detect cysteine based on

fluorescence enhancement or quenching at single emission wavelength, which may be influenced by various variable factors including excitation intensity, emission collection efficiency, probe concentration and environmental effects.^{40,41} In contrast, ratiometric fluorescent probes could be applied to resolve this problem, which can offer a built-in calibration by simultaneously measuring fluorescence intensities at two different emission wavelengths.^{42,43} Fluorescence resonance energy transfer (FRET) process is widely used in the construction of ratiometric fluorescent probes because of its large pseudo-Stokes shift and small spectral overlap, which can better distinguish the dual emission wavelengths.^{44,45} But, only few fluorescence resonance energy transfer (FRET)-based ratiometric fluorescent probe for detecting cysteine have been reported.^{46,47} Therefore, FRET-based ratiometric fluorescent probes for highly selective detection of cysteine are extremely demanded for further researching the roles of cysteine.

In this article, a FRET-based ratiometric fluorescent probe for highly selective detection of cysteine was designed and synthesized. A coumarin derivative with excellent optical properties and high fluorescence quantum yield was used as an energy donor, a rhodol derivative was applied as an energy acceptor, and an acrylate group was utilized as a cysteine recognition group. When there is no cysteine, the rhodol energy receptor is in a non-fluorescent spirolactone form and the FRET process of the probe remains off. So, free probe displays inherent blue fluorescence of coumarin chromophore. However, in the presence of cysteine the probe undergoes a Michael addition and intermolecular cyclization reaction, and the closed spirolactone form was converted to a conjugated fluorescent xanthene form to trigger the occurrence of FRET which resulted in a fluorescent signal decrease at 470

89 nm and enhancement at 543 nm. The ratiometric fluorescent probe exhibited highly selectivity
90 toward cysteine over Hcy and GSH. Moreover, the probe showed low cell toxicity and had
91 been successfully applied to the confocal imaging of cysteine in HepG2 cells by dual
92 emission channels.

93 2. Experimental

94 2.1. Materials and instruments

95 4-(Diethylamino)salicylaldehyde, diethyl malonate, *m*-diphenol, phthalic anhydride,
96 trifluoroacetic acid, 4-diaminopyridine (DMAP), acryloyl chloride were purchased
97 from Heowns Biochemical Technology Company.
98 1-Ethyl-3-(3-dimethylaminopropyl)carbodiimide hydrochloride (EDC) and
99 *m*-hydroxyphenylpiperazine were purchased from Energy Chemical (Shanghai, China).
100 Cysteine (Cys) and homocysteine (Hys) were purchased from TCI (Shanghai) Development
101 Company. Glutathione (GSH) is purchased from Aladdin Reagent Company. Threonine (Thr),
102 leucine (Leu), methionine (Met), valine (Val), phenylalanine (Phe), serine (Ser), asparagine
103 (Asn), tryptophan (Trp), tyrosine (Tyr), glutamine(Gln), lysine (Lys), isoleucine (Ile), alanine
104 (Ala), histidine (His), aspartic acid (Asp), arginine (Arg), proline (Pro), glutamic acid (Glu)
105 and glycine (Gly) were obtained from Shanghai Lanji Science and Technology Development
106 Company. Anhydrous aluminum chloride and *n*-hexane were purchased from Tianjin Sailboat
107 Chemical Reagent Technology Company. Nitrobenzene was purchased from Tianjin Damao
108 Chemical Reagent Factory. Hexahydropyridine was purchased from Shanghai Pharmaceutical
109 Reagent Company of China Pharmaceutical Group. Triethylamine was purchased from
110 Tianjin Fuchen Chemical Reagent Factory. The solvents used in the high performance liquid

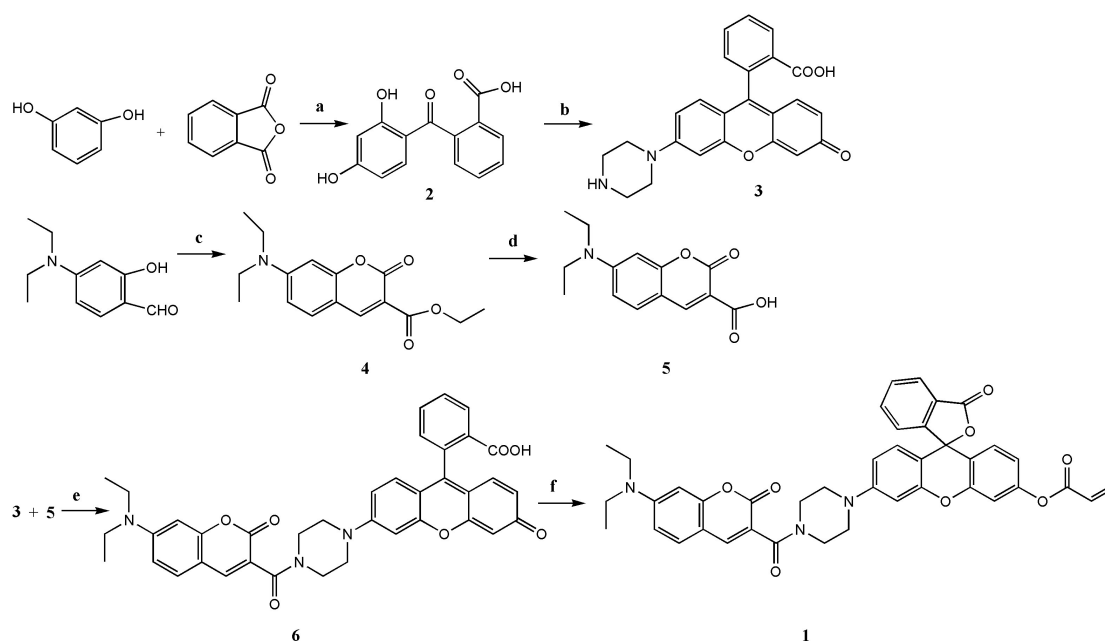
chromatography (HPLC) experiments were all chromatographically pure and purchased from Tianjin Siyou Fine Chemicals Company. All other chemical reagents were analytically pure reagents, purchased from commercial suppliers and used directly in the experiment without further purification. Thin layer chromatography was performed using silica gel 60 F254, and column chromatography was conducted on silica gel (200-300 mesh), both of which were purchased from China Qingdao Ocean Chemical. Water is purified by SZ-93 automatic double pure water distiller (Shanghai Yarong Biochemical Instrument Factory).

The NMR spectrum was recorded with Bruker's DRX-500 spectrometer using tetramethylsilane (TMS) as an internal standard. Mass spectra were obtained on an Agilent Technologies 6420 Triple Quad LC/MS high resolution mass spectrometer. All fluorescence tests were performed on a Hitachi F-7000 fluorescence spectrophotometer with a 1 cm quartz absorption cell with an excitation wavelength of 418 nm and an entrance and exit slit of 10 nm. The UV-visible absorption spectrum was measured by an EVOLUTION 260 BIO UV-Vis spectrophotometer with a 1 cm quartz absorption cell. The pH was measured by a pH meter (METTLER TOLEDO Fiveeasy Plus). The DF-101S collector-type constant-temperature heating magnetic stirrer produced by Gongyi City Yuhua Instrument Company and the MS-PB magnetic stirrer manufactured by Shanghai Yuhuai Instrument Company were used in the synthesis process. High performance liquid chromatograms were obtained with an UltiMate 3000 high performance liquid chromatograph equipped with an XBP-C18 column (5 μ m, 4.6 \times 250 mm). Fluorescence imagings of living cells were recorded by an Olympus FV-1200 single photon laser confocal microscope. Data processing is mainly obtained in SigmaPlot software. The data obtained by fluorescence spectrophotometry and

UV-visible spectrophotometry were measured in 0.01 mol/L PBS buffer ($\text{CH}_3\text{CN}/\text{water} = 6.4$,
 V/V, pH = 7.40). In addition to the fluorescence data obtained by time scanning, all other
 fluorescence and absorption data were recorded at 60 min after addition of cysteine at room
 temperature.

2.2. Syntheses

The synthetic route for FRET-based ratiometric fluorescence probe **1** for highly selective
 detection of cysteine is shown in Scheme 1. The probe **1** uses a coumarin-rhodol fluorescence
 resonance energy transfer system as a mechanism. Fluorescence emission spectrum of
 coumarin energy donor (compound **5**) efficiently overlaps with the UV-vis absorption
 spectrum of rhodol energy acceptor (compound **3**), indicating that FRET process would occur
 to induce the appearance of acceptor emission concomitant with disappearance of donor
 emission (Figure 1).



Scheme 1 Synthesis of FRET-based ratiometric fluorescent probe **1**: (a) nitrobenzene,
 anhydrous AlCl_3 , 84%; (b) *m*-hydroxyphenylpiperazine, CF_3COOH , 75%; (c) diethyl

malonate, hexahydropyridine, 81%; (d) I . NaOH, II . HCl , 75%; (e) EDC, DMAP, 43%, (f)
 anhydrous CH_2Cl_2 , triethylamine, acryloyl chloride, 61%.

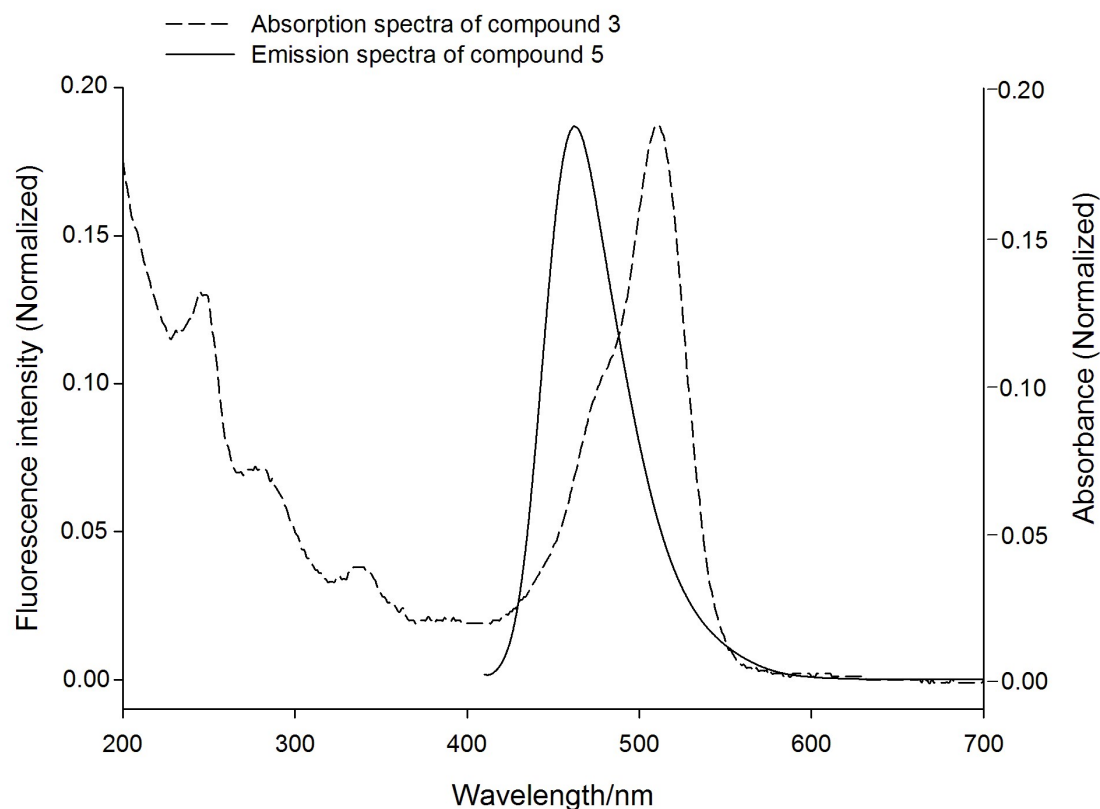


Figure 1 Normalized emission spectra of donor derivative 5 (5.0 μM) and normalized absorption spectra of acceptor 3 (5.0 μM) in 0.01 M PBS buffer ($\text{CH}_3\text{CN}/\text{water} = 6:4$, V/V, pH=7.40). The medium dash (---) and solid line (—) represent normalized absorption of compound 3 and normalized emission spectra of compound 5, respectively.

Synthesis of compound 2. The compound 2 is synthesized according to the reported document.⁴⁵ Under a nitrogen stream, resorcinol (0.55 g, 5 mmol) and phthalic anhydride (0.74 g, 5 mmol) were dissolved in 30 ml of nitrobenzene, and then anhydrous AlCl_3 (1.47 g, 11mmol) was added, and the reaction was stirred at room temperature for 12 h. The reaction mixture was poured into a two-phase solution of vigorously stirred 30 ml *n*-hexane and 40 ml 0.5 M HCl. After the reaction was stirred for 2 h, an orange-yellow precipitate was obtained

161 and filtered to give a crude product. Then The product was purified through column
162 chromatograph using dichloromethane/methanol (15:1, v/ v) as the eluent to obtain compound
163 2 as an orange solid (1.08 g, 84%). ¹H NMR (500 MHz, CD₃OD), δ(ppm): 8.06 (1H, d, *J* = 7.7
164 Hz), 7.65 (1H, t, *J* = 7.5 Hz), 7.59 (1H, t, *J* = 7.5 Hz), 7.34 (1H, d, *J* = 7.5 Hz), 6.93 (1H, d, *J*
165 = 8.8 Hz), 6.31 (1H, d, *J* = 2.0 Hz), 6.21(1H, dd, *J* = 8.8 Hz, 2.0 Hz).

166 **Synthesis of Compound 3.** The compound 3 is synthesized according to the reported
167 document.⁴⁵ Compound 2 (1.03 g, 4 mmol) was dissolved in 20 ml of CF₃COOH and then
168 *m*-hydroxyphenylpiperazine (0.71 g, 4mmol) was also added into the above mixture. This
169 reaction mixture was heated to reflux for 36 h, then the solvent was removed under reduced
170 pressure. It was further purified by column chromatograph using dichloromethane/methanol
171 (5:1, v/v) to obtain a red solid compound 3 (1.21 g, 75%). ¹H NMR (500 MHz, DMSO-*d*₆),
172 δ(ppm): 10.22 (1H, s), 7.99 (1H, d, *J* = 7.7 Hz), 7.80-7.77 (1H, m), 7.72-7.69 (1H, m), 7.24
173 (1H, d, *J* = 7.6 Hz), 6.89 (1H, d, *J* = 2.3 Hz), 6.76 (1H, dd, *J* = 8.9 Hz, 2.3 Hz), 6.68 (1H, s),
174 6.58-6.55 (3H, m), 3.44 (4H, d, *J* = 5.3 Hz), 3.21 (4H, d, *J* = 4.8 Hz).

175 **Synthesis of compound 4.** Synthesis of compound 4 according to reported literature.⁴⁵
176 4-(Diethylamino)salicylaldehyde (0.97 g, 5 mmol) was dissolved in 25 ml CH₃CH₂OH, then
177 diethyl malonate (0.96 g, 6 mmol) and 0.5 ml hexahydropyridine were added. The reaction
178 mixture was stirred under reflux for 2 h, diluted with 50 ml water, extracted with ethyl acetate
179 (50 ml × 3), and dried over anhydrous MgSO₄. The solvent was removed under reduced
180 pressure and the crude product was purified by column chromatography using petroleum
181 ether/ethyl acetate (3:1, v/v) to get an orange compound 4 (1.16 g, 81%). ¹H NMR (500MHz,

CDCl₃), δ (ppm): 8.40 (1H, s), 7.33 (1H, d, J =8.9 Hz), 6.57 (1H, dd, J = 8.9 Hz, 2.2 Hz), 6.43 (1H, d, J = 2.1 Hz), 4.34 (2H, q, J = 7.1 Hz), 3.42 (4H, q, J = 7.1 Hz), 1.36 (3H, t, J = 7.1 Hz), 1.20 (6H, t, J = 7.1 Hz).

Synthesis of compound 5. Synthesis of compound 5 according to reported literature.

⁴⁵Compound 4 (1.05 g, 4 mmol) was dissolved in 40 ml ethanol and then 40 ml 0.5 M NaOH was added. This mixture was stirred at room temperature for 12 h. The solvent was evaporated under reduced pressure to give a solid. The solid was dissolved in 5 ml water, and the pH of the solution was acidified with 1M HCl to give a precipitate. When the precipitate was filtered, a red-brown solid compound 5 (0.78 g, 75%) was obtained. ¹H NMR (500MHz, CDCl₃), δ (ppm): 12.30 (1H, s), 8.64 (1H, s), 7.44 (1H, d, J = 9.1 Hz), 6.69 (1H, dd, J = 9.1 Hz, 2.4 Hz), 6.51 (1H, d, J = 2.4 Hz), 3.47 (4H, q, J = 7.2 Hz), 1.24 (6H, t, J = 7.2 Hz).

Synthesis of compound 6. Under nitrogen protection, compound 3 (0.40 g, 1 mmol) was dissolved in 60 ml anhydrous dichloromethane/anhydrous *N,N*-dimethylformamide (5:1, v/ v). Then DMAP (0.06 g, 0.5 mmol) and EDC (0.19 g, 1 mmol) were added. Then the mixture was stirred at room temperature for 30 min. Compound 5 (0.31 g, 1.2 mmol) was added and stirred overnight. The reaction solution was evaporated under reduced pressure to give a crude product. Then it was further purified by column chromatograph using dichloromethane/methanol (20:1, v/ v) as the eluent to get a red compound 6 (0.28 g, 43%).

¹H NMR (500 MHz, DMSO-*d*₆), δ (ppm): 10.10 (1H, s), 8.00-7.97 (2H, m), 7.77 (1H, d, J = 7.5 Hz), 7.71 (1H, d, J = 7.5 Hz), 7.49 (1H, d, J = 8.9 Hz), 7.25 (1H, d, J = 7.6 Hz), 6.81 (1H, s), 6.74 (2H, d, J = 9.0 Hz), 6.66 (1H, s), 6.54 (4H, d, J = 7.0 Hz), 3.69 (2H, s), 3.45-3.42 (6H, m), 3.32 (2H, d, J = 1.1 Hz), 3.25 (2H, s), 1.12 (6H, t, J = 7.0 Hz). MS (ESI) *m/z*: 644.1000

204 (M+H)⁺, 666.1000 (M+Na)⁺.

205 **Synthesis of compound 1.** Compound 6 (0.64 g, 1mmol) was dissolved in 20 ml anhydrous
206 dichloromethane followed by addition of 1.4 ml triethylamine, then acryloyl chloride (0.18 g,
207 2 mmol) was added slowly. After half an hour of reaction at 0°C, the reaction was stirred at
208 room temperature for 12 h. Subsequently, the solvent was evaporated under reduced pressure.
209 The crude product was further purified by column chromatograph using
210 dichloromethane/methanol (30:1, v/ v) as the eluent to obtain a yellow compound 1 (0.43 g,
211 61%). ¹H NMR (500 MHz, CDCl₃), δ(ppm): 7.98 (1H, d, *J* = 7.6 Hz), 7.86 (1H, s), 7.64 (1H, t,
212 *J* = 7.4 Hz), 7.58 (1H, t, *J* = 7.4 Hz), 7.27 (1H, d, *J* = 8.8 Hz), 7.15 (1H, d, *J* = 7.6 Hz),
213 7.08-7.07 (1H, m), 6.80-6.76 (2H, m), 6.68 (1H, d, *J* = 1.9 Hz), 6.64-6.56 (4H, m), 6.44 (1H,
214 d, *J* = 1.9 Hz), 6.28 (1H, dd, *J* = 17.3 Hz, 10.5 Hz), 6.01 (1H, d, *J* = 10.5 Hz), 3.86 (2H, s),
215 3.54 (2H, s), 3.40 (4H, q, *J* = 7.0 Hz), 3.30 (4H, d, *J* = 16.6 Hz), 1.19 (6H, t, *J* = 7.0 Hz). ¹³C
216 NMR (125 MHz, CDCl₃), δ(ppm): 169.29, 165.02, 163.88, 159.09, 157.26, 152.90, 152.52,
217 152.12, 151.94, 151.71, 151.69, 145.39, 135.00, 133.17, 129.86, 129.72, 128.95, 128.70,
218 127.45, 126.50, 124.94, 123.96, 117.11, 116.82, 115.76, 112.33, 110.17, 109.35, 109.21,
219 107.66, 102.35, 96.83, 82.60, 48.40, 47.95, 46.77, 44.87, 41.88, 12.33. MS (ESI) *m/z*:
220 698.2000 (M+H)⁺, 702.2000 (M+Na)⁺. In the DEPT135 spectrum, the chemical shift of 82.60
221 corresponds to the carbonyl carbon of spirolactone, indicating that compound 1 was in a
222 spirolactone form.

223 2.3. Cytotoxicity assay

224 Cytotoxicity is an important indicator of the performance of fluorescent probe bioimaging
225 applications. In order to detect the cytotoxicity of the probe,

3-(4,5-dimethylthiazole-2)-2,5-diphenyltetrazolium bromide (MTT) colorimetric method was used. The selected cells were HepG2 cells (liver cancer cells). First, the HepG2 cells were cultured in 10% fetal bovine serum medium, about 1×10^4 cells were seeded in each well of a 96-well plate and the total volume per well was controlled at 100 μL . After the HepG2 cells was placed in an incubator containing 5% CO_2 at 37°C for 24 h, the medium was aspirated. Then, the HepG2 cells were incubated with different concentrations of compound 1 and compound 6 with fresh medium for 4 h. After that, the medium was removed from this 96-well plate and added to the fresh medium for 24 h. The HepG2 Cells were incubated with the fresh medium (100 μL) containing MTT (10 μL , 5 mg mL^{-1}) for 4 h. At last, the supernatant in the 96-well plate was aspirated and 150 μL DMSO was participated, shaken for 10 min. Then the absorbance at 490 nm was measured with a microplate reader and cell viability was estimated by $A/A_0 \times 100\%$ (A and A_0 are the absorbance of experimental group and control group, respectively).

2.4. Confocal imaging in living cells

The HepG2 cells were cultured on the laser confocal culture dishes at 37°C for 24 h to ensure good cell growth, and then washed three times with Dulbecco's phosphate buffered saline (DPBS). In a control experiment, HepG2 cells were pretreated with 1 mM *N*-methylmaleimide (sulfhydryl masking agent) for 40 min, washed three times with DPBS. Then HepG2 cells were incubated with 10 μM probe 1 for 45 min, rinsed with DPBS three times and imaged. In the experimental group of imaging endogenous Cys, HepG2 cells were treated with 10 μM probe 1 for 45 min, after which the cells were washed with DPBS three times and imaged. In the experimental group of imaging exogenous Cys, HepG2 cells were

incubated with 10 μM probe 1 for 45 min and washed three times with DPBS, after which the cells were incubated with 0.1 mM Cys for another 45 min, washed three times with DPBS and imaged. Confocal fluorescence images were observed by an Olympus FV1200-MPE multiphoton confocal microscope with 60 \times objective lens.

3. Results and discussion

3.1. Spectroscopic analytical performance of probe 1 towards Cys

In presence of 100 μM cysteine, the probe can exhibit better fluorescence sensing for cysteine (Figure S1). So, 60% organic solvents in buffer solution was used in the experiment. To study the fluorescence sensing properties of probe 1 for Cys, we investigated the change of fluorescence response of probe 1 (10 μM) to 0.01 M PBS buffer (CH_3CN : water = 6:4, v/v, pH = 7.40) containing different amounts of Cys (Figure 2). From Figure 2, when there is no cysteine, probe 1 exhibited strong fluorescence with an emission peak at 470 nm. However, in the presence of incremental Cys (0-100 μM), the initial fluorescence at 470 nm decreased gradually, a new fluorescence emission peak appeared at 543 nm and increased progressively, permitting a ratiometric fluorescence response for Cys. It is remarkable that the large emission shift ($\Delta\lambda = 73$ nm) results in two well-resolved emission bands for the probe, which would be beneficial for dual-channel imaging of Cys in biological samples with less cross-talk observed. The notable change in fluorescence spectra should be attributed to Cys-induced occurrence of FRET between the donor coumarin and acceptor rhodol. FRET efficiency is an important parameter of the FRET dye, which indicates the energy transfer efficiency between the donor and the acceptor. The fluorescence emission intensities of compound 5 (10 μM) and the reaction product of fluorescent probe 1 (10.0 μM) with cysteine

(100 μM) at 470 nm were 8222 and 862 (Figure S2), so the fluorescence resonance energy transfer efficiency was estimated to be 89.5% according to Energy Transfer Efficiency (ETE)

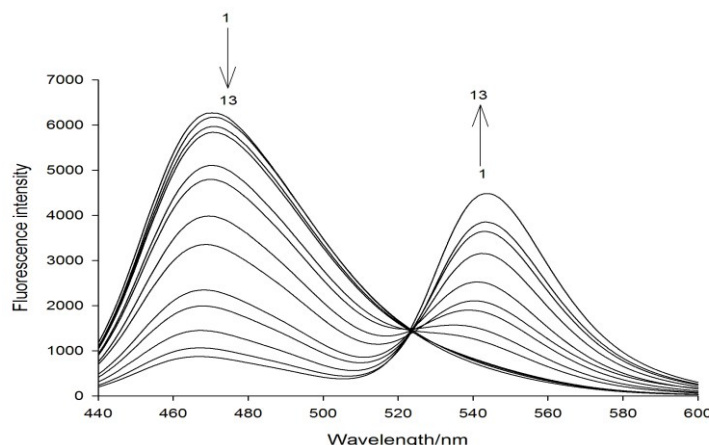
$$= \left[\frac{\text{fluorescence of donor} - \text{fluorescence of donor in cassette}}{\text{fluorescence of donor}} \right] \times 100\%.^{48}$$


Figure 2 One-photon fluorescence spectra of probe 1 (10.0 μM) in the presence of various concentrations of cysteine: 0, 0.5, 0.7, 1.0, 3.0, 5.0, 7.0, 10, 20, 30, 50, 70, 100 μM from 1 to 13 ($\lambda_{\text{ex}} = 418 \text{ nm}$).

We further studied the UV-vis absorption spectra of probe 1 (10 μM), the reaction mixture of fluorescent probe 1 (10 μM) with cysteine (100 μM), and compound 6 (10 μM) (Figure 3). From Figure 3, Probe 1 has a maximum absorption at 407 nm, which corresponds to absorption of the coumarin donor,⁴⁹ and compound 6 absorbs at both 407 nm and 511 nm. In the presence of cysteine, no obvious absorption changes of the donor occurred, while a new absorption peak at 511 nm belonging to the conjugated xanthene form of the acceptor emerged.⁵⁰ The above results indicates that the reaction of the probe 1 with cysteine yields the compound 6.

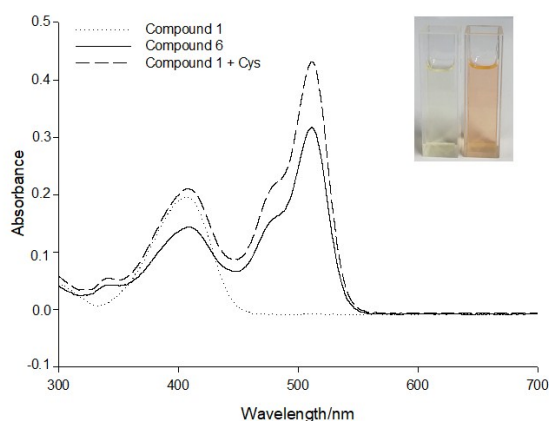


Figure 3 Absorption spectra of fluorescent probe **1** (10 μM), compound **6** (10 μM), and the reaction mixture of fluorescent probe **1** (10 μM) with cysteine (100 μM). The dotted line (\cdots), solid line ($—$), and medium dash ($- -$) represent fluorescent probe **1**, compound **6** and the reaction product of fluorescent probe **1** with cysteine, respectively. Inset: color changes in probe **1** upon addition of cysteine.

3.2. Principle of operation and the basis of quantitative assay

In order to investigate the linear response of the ratio value of the emission intensities at 543 nm and 470 nm ($I_{543\text{nm}}/I_{470\text{nm}}$) toward Cys, we chose different concentrations of Cys for experiments. When the concentration of cysteine was 5.0×10^{-7} – 1.0×10^{-4} mol L^{-1} (Figure 4), the ratio of $I_{543\text{nm}}/I_{470\text{nm}}$ was linear with the concentration of Cys. The linear regression equation was $I_{543\text{nm}}/I_{470\text{nm}} = 0.0763 + 0.0507 \times 10^6 \times C$ ($R = 0.9997$), C is the concentration of cysteine, and R is the linear correlation coefficient. The detection limit was calculated by $3S_B/m$, S_B is the standard deviation of the fluorescence intensity measured 10 times for the blank solution, and m is the slope of the calibration curve.⁴⁹ The limit detection of probe **1** for cysteine was 2.0×10^{-7} mol L^{-1} , which is much lower than previously reported ratiometric

fluorescent probe for Cys.^{46, 51-53} The results indicate that probe 1 can be used for highly sensitive quantitative detection of cysteine.

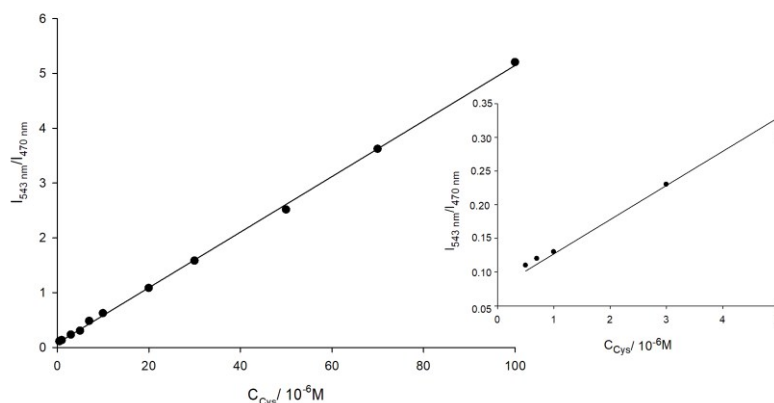
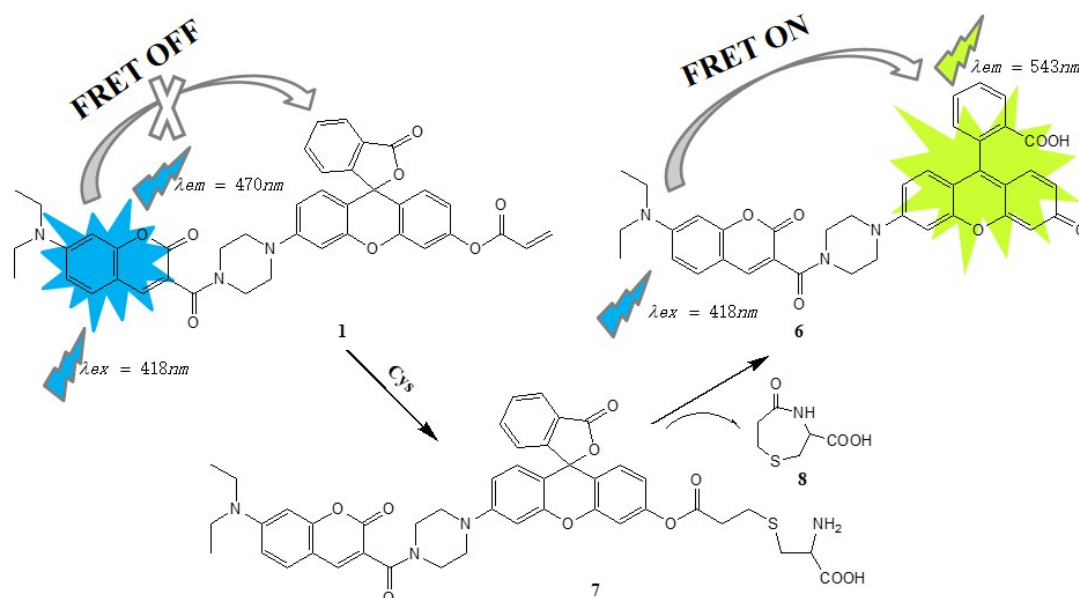


Figure 4. Fluorescence intensity ratio ($I_{543\text{ nm}}/I_{470\text{ nm}}$) of probe 1 (10 μM) as a function of the concentration of cysteine from 0.5 μM to 100 μM . The inset exhibits the corresponding fluorescence intensity ratio ($I_{543\text{ nm}}/I_{470\text{ nm}}$) of probe 1 (10 μM) as a function of the concentration of cysteine from 0.5 μM to 5.0 μM .

The response mechanism of probe 1 to cysteine may be ascribed to the reaction of probe 1 with Cys to produce compound 6 (Scheme 2). As displayed in Scheme 2, in the absence of cysteine, the rhodol receptor was in the non-fluorescent lactone state and FRET process was inhibited. Upon addition of cysteine, a Michael addition reaction was taken place between acryloyl group of probe 1 and thiol group of Cys to generate thioether compound 7. Subsequently, compound 7 underwent an intramolecular cyclization to produce compound 6 accompanied by the release of the cyclization product 8. Thus, in the presence of cysteine, the closed spirolactone form was converted to a conjugated fluorescent xanthenes form to induce the occurrence of FRET. In order to further verify the reaction mechanism of probe 1 for cysteine, we performed HPLC on probe 1, reaction mixture of probe 1 with Cys and

compound 6 (Figure 5). As shown in Figure 5, probe 1 peaked at 6.65 min, the reaction mixture of probe 1 with cysteine showed a peak after 2.98 min of injection, which was consistent with the retention time of compound 6 in the HPLC. The ESI-MS data of reaction mixture of probe 1 with Cys for 10 min displayed signal at 642.2215 and 819.0283, respectively (Figure S3). As illustrated in Figure S3, the signal at 642.2215 was consistent with the structure [compound 6 - H]⁺ and the signal at 819.0283 was attributed to the structure [compound 7 + H]⁺. Simultaneously, in the ultraviolet absorption spectrum property, the maximum absorption wavelength of the compound 6 and the reaction mixture of probe 1 with cysteine was identical. Therefore, it can be proved that the response mechanism of probe 1 to cysteine was presumed to be correct.



328

329 Scheme 2. Proposed possible mechanism of the response of compound 1 to cysteine

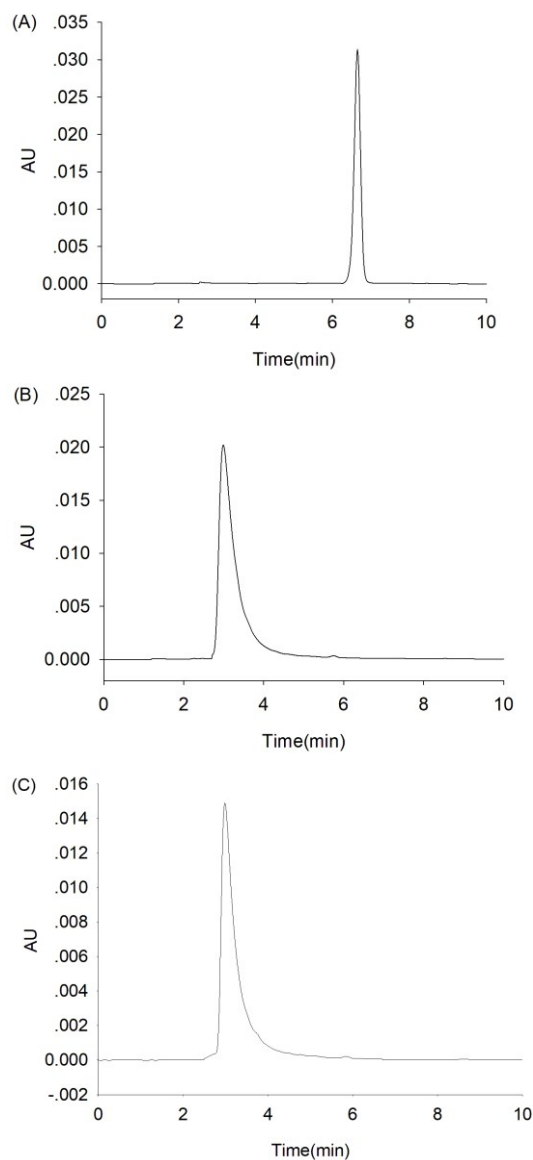


Figure 5. HPLC profiles of (A) compound 1 (10 μM), (B) compound 6 (10 μM) and (C) the reaction mixture of compound 1 (10 μM) with cysteine (100 μM). HPLC conditions: 1.0 mL/min total flow rate, Agela Technologies Venusil XBP-C18: 5 μm , 4.6 \times 250 mm column, isocratic elution with acetonitrile at flow rate 0.8 mL/min and water at flow rate 0.2 mL/min, detected at 407 nm.

3.3. Time-dependent responses and effect of pH

We further investigated the time response of probe 1 (10 μ M) under conditions of addition of Cys (100 μ M) (Figure S4). Figure S4 showed the trend of the value of $I_{543\text{ nm}}/I_{470\text{ nm}}$ over time. When Cys (100 μ M) was added, the value continues to increase and reached a maximum and saturate at 60 min. The experimental results showed that probe 1 is stable under the experimental conditions, and the detection of cysteine can be completed within 60 min. In this study, an assay time of 60 min was chosen as the optical measurement condition.

In order to test the sensitivity of synthesized probe 1, we studied changes in the $I_{543\text{ nm}}/I_{470\text{ nm}}$ values of synthesized probe 1 (10 μ M) before and after adding Cys (100 μ M) at different pH values (Figure 6). As depicted in Figure 6, the probe 1 has good sensitivity to the Cys at a pH range of 6.00-11.50. Therefore, experimental results showed that probe 1 can work in a large pH range and can be used for biological detection.

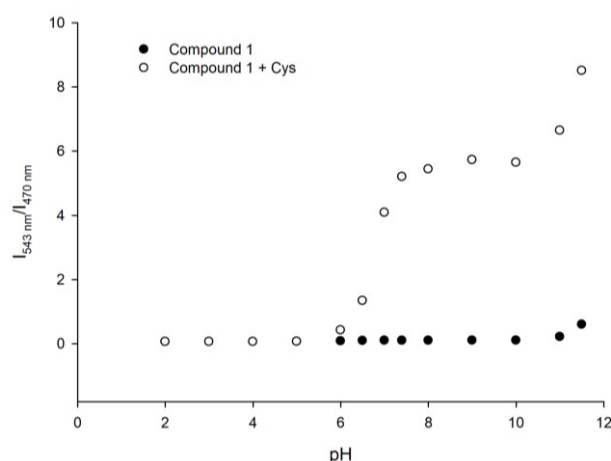


Figure 6. Effect of pH on the ratio of fluorescence intensity ($I_{543\text{ nm}}/I_{470\text{ nm}}$) of 10 μ M probe 1 in the absence (filled circles) and presence of 100 μ M cysteine (clear circles). All data were obtained at various pH values (pH 2.00-11.50).

3.4. Selectivity

An important indicator for evaluating the performance of fluorescent probe for target sensing is selectivity. We studied the fluorescence response of probe 1 to cysteine and other related substances at pH 7.40 (Figure 7A). As shown in Figure 7A, in the presence of cysteine probe 1 showed significant fluorescence enhancement, while the addition of other substances had little effect on the fluorescence of probe 1. To investigate the potential applications of probes in complex biological samples, we also investigated the effect of coexistence of other substances and cysteine on the sensitivity of fluorescent probe to cysteine at a pH of 7.40 (Figure 7B). From Figure 7B, the probe still maintains a fluorescent response to cysteine in the presence of other related substances.

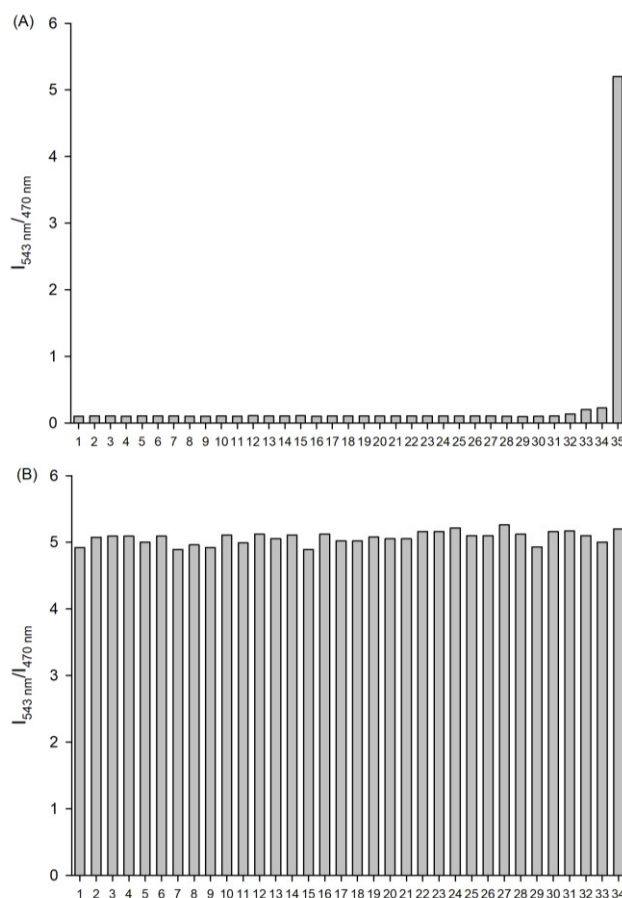


Figure 7. (A) Fluorescence response of probe 1 (10 μM) toward Cys and other substances at pH 7.40: (1) blank, (2) Thr, (3) Leu, (4) Met, (5) Val, (6) Phe, (7) Ser, (8) Asn, (9) Trp, (10) Tyr, (11) Gln, (12) Lys, (13) Ile, (14) Ala, (15) His, (16) Asp, (17) Arg, (18) Pro, (19) Glu, (20) Gly, (21) F^- , (22) CO_3^{2-} , (23) CH_3COO^- , (24) $\text{S}_2\text{O}_3^{2-}$, (25) NO_2^- , (26) SO_4^{2-} , (27) Cl^- , (28) NO_3^- , (29) I^- , (30) Br^- , (31) SCN^- , (32) SO_3^{2-} , (33) Hcy, (34) GSH, (35) Cys; (B) Fluorescence response of probe 1 (10 μM) toward Cys in the presence of other substances at pH 7.40: (1) Thr, (2) Leu, (3) Met, (4) Val, (5) Phe, (6) Ser, (7) Asn, (8) Trp, (9) Tyr, (10) Gln, (11) Lys, (12) Ile, (13) Ala, (14) His, (15) Asp, (16) Arg, (17) Pro, (18) Glu, (19) Gly, (20) F^- , (21) CO_3^{2-} , (22) CH_3COO^- , (23) $\text{S}_2\text{O}_3^{2-}$, (24) NO_2^- , (25) SO_4^{2-} , (26) Cl^- , (27) NO_3^- , (28) I^- , (29) Br^- , (30) SCN^- , (31) SO_3^{2-} , (32) Hcy, (33) GSH, (34) Cys. The concentration of all substances added to probe 1 is 100 μM .

3.5. Cytotoxicity assays and confocal imaging in living cells

We tested cytotoxicity of probe 1 and compound 6 at different concentrations (0, 2, 4, 8, 16 μM) against HepG2 cells by MTT assay (Figure 8). As depicted in Figure 8, when probe 1 and compound 6 were present, cell viability reached 80% or more, which indicates that probe 1 and compound 6 were almost non-toxic to HepG2 cells.

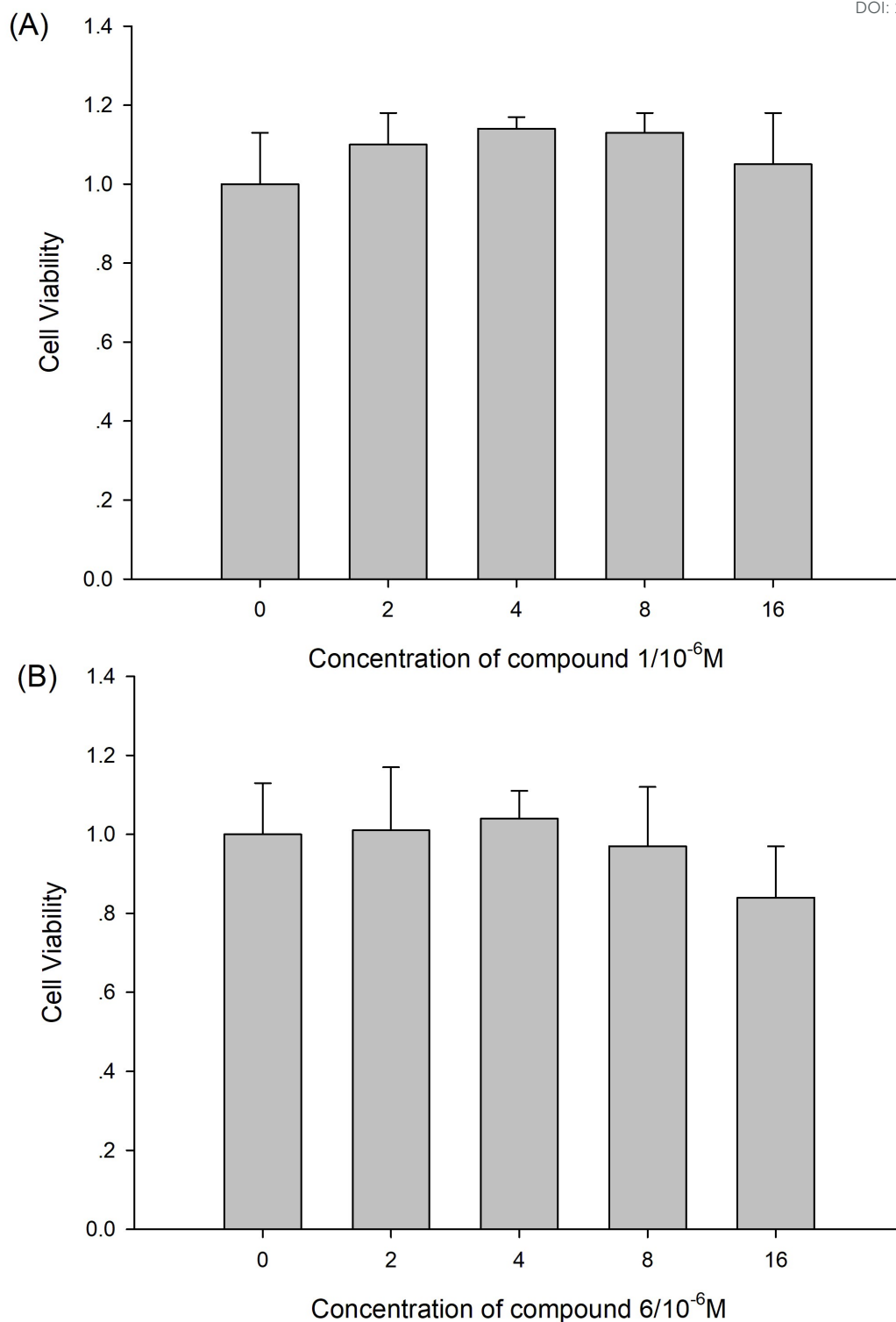


Figure 8. MTT assay of HepG2 cells in the presence of different concentrations of compound 1 (a) and compound 6 (b) (0, 2, 4, 8, 16 μM) for 24 h at 37 $^{\circ}\text{C}$, respectively.

In order to demonstrate the practicality of probe 1 in biology, we performed laser confocal fluorescence imaging of cysteine in HepG2 cells with fluorescent probe 1 (Figure 9). HepG2

cells were seeded in three 35mm laser confocal culture dishes and incubated for 24 h. The HepG2 cells was pretreated with 1 mM *N*-methylmaleimide (sulfhydryl masking agent) for 40 min, and incubated with 10 μ M probe 1 medium for 45 min for fluorescence imaging, it was found that the blue channel has obvious fluorescence (Figure 9b), and the red channel has almost no fluorescence (Figure 9 c). In the control experiment, HepG2 cells were incubated in a medium containing 10 μ M probe 1 for 45 min for fluorescence imaging. The results showed that the blue channel showed weak fluorescence (Figure 9 f) and the red channel was more obvious fluorescence (Figure 9 g). Simultaneously, HepG2 cells were incubated with 10 μ M probe 1 for 45 min, then incubated with 0.1 mM Cys for 45 min and imaged. The experimental results exhibited that the fluorescence of the blue channel was weak (Figure 9 j), and the fluorescence of the red channel was stronger than that without added Cys (Figure 9 k). These phenomena indicate that the probe 1 can be used for the ratiometric dual-channel detection of cysteine in living cells.

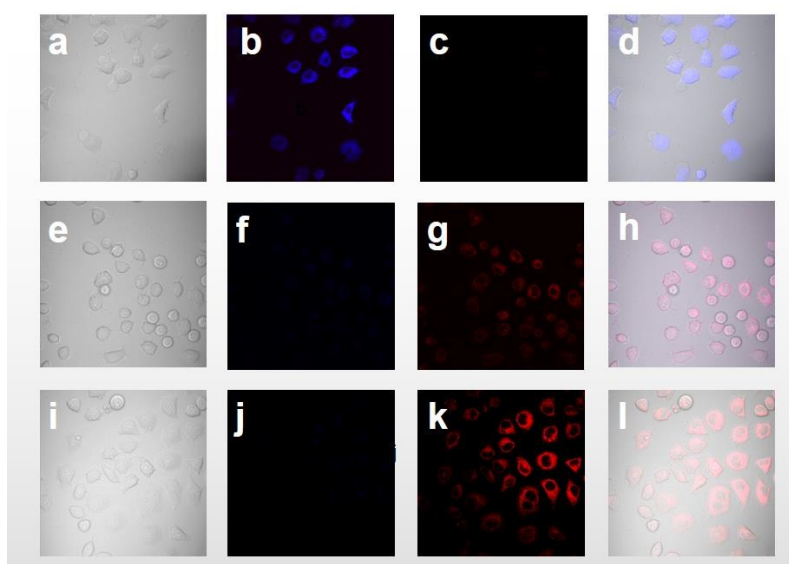


Figure 9. Laser confocal fluorescence imaging of cysteine in HepG2 cells with fluorescent probe 1. (a) Bright field image after incubation of HepG2 cells with 1 mM

400 *N*-methylmaleimide for 40 min, and incubation of HepG2 cells with 10 μ M probe for 1 45
401 min; (b) fluorescence image from blue channel of image (a); (c) fluorescence image from red
402 channel of image (a); (d) overlay image of (a), (b) and (c); (e) Bright field map after
403 incubation of HepG2 cells for 45 min with 10 μ M probe 1; (f) fluorescence image from blue
404 channel of image (e); (g) fluorescence image from red channel of image (e); (h) overlay
405 image of (e), (f) and (g); (i) bright field images of HepG2 cells incubated with probe 1 for 45
406 min, then with 10 μ M Cys for 45 min; (j) fluorescence image from blue channel of image (i);
407 (k) fluorescence image from red channel of image (i); (l) overlay image of (i), (j) and (k).

408 4. Conclusions

409 In summary, we designed and synthesized a FRET-based ratiometric probe for detection of
410 Cys based on a coumarin-rhodol derivative. An acrylate group was applied as an identification
411 group for Cys. In the absence of cysteine, the rhodol receptor was in the non-fluorescent
412 lactone state and FRET process was inhibited. Upon addition of cysteine, the closed
413 spirolactone form was converted to a conjugated fluorescent xanthenes form to induce the
414 occurrence of FRET which resulted in a fluorescent signal decrease at 470 nm and
415 enhancement at 543 nm. The probe shows high sensitivity and selectivity for cysteine over
416 glutathione, homocysteine, and other related substances. In addition, the probe also has good
417 cell permeability and has been successfully applied for the ratiometric dual-channel detection
418 of cysteine in living cells.

419 Conflicts of interest

420 There are no conflicts of interest to declare.

421 Acknowledgments

This work was supported by the Key Science and Technology Programme of Henan Province (182102310101), National Natural Science Foundation of China (Grant nos. 21807027 and 81130062), the Fundamental Research Funds for the Provincial Universities (2014KYYWF-QN04), and Graduate Innovation Fund in Henan College of Chinese Medicine (YJS2018A05).

References

- 1 X. Chen, Y. Zhou, X. Peng and J. Yoon, *Chem. Soc. Rev.*, 2010, **39**, 2120.
- 2 Y. Yang, Q. Zhao, W. Feng and F. Li, *Chem. Rev.*, 2013, **113**, 192.
- 3 D. M. Townsend, K. D. Tew and H. Tapiero, *Biomed. Pharmacother.*, 2003, **57**, 145.
- 4 K. G. Reddie and K. S. Carroll, *Curr. Opin. Chem. Biol.*, 2008, **12**, 746.
- 5 E. Weerapana, C. Wang, G. M. Simon, M. B. D. Dillon, D. A. Bachovchin, K. Mowen, D. Baker and B. F. Cravatt, *Nature*, 2010, **468**, 790.
- 6 A. K. Elshorbagy, V. Kozich, A. D. Smith and H. Refsum, *Curr. Opin. Clin. Nutr. Metab. Care*, 2012, **15**, 49.
- 7 M. T. Heafield, S. Fearn, G. B. Steventon, R. H. Waring, A. C. Williams and S. G. Sturman, *Neurosci. Lett.*, 1990, **110**, 216.
- 8 R. Janáky, V. Varga, A. Hermann, P. Saransaari and S. S. Oja, *Neurochem. Res.*, 2000, **25**, 1397.
- 9 X. F. Wang and M. S. Cynader, *J. Neurosci.*, 2001, **21**, 3322.
- 10 W. Zhang, P. Li, Q. Geng, Y. Duan, M. Guo and Y. Cao, *J. Agric. Food Chem.*, 2014, **62**, 5845.
- 11 Y. Wang, C. H. Zhang, Y. H. Zheng, Y. Ge, X. Y. Yu, *Anal. Lett.*, 2019, **52**, 1487.

- 444 12 A. V. Ivanov, E. D. Virus, B. P. Luzyanin and A.A. Kubatiev, *J. Chromatogr. B.*, 2015,
445 **1004**, 30.
- 446 13 R. C. de Carvalho, T. R. D. Mathias, A. D. P. Netto, F. F. D. Marques, *Electrophoresis*,
447 2018, **39**, 1613.
- 448 14 N. Shao, J. Y. Jin, S. M. Cheung, R. H. Yang, W. H. Chan and T. Mo, *Angew. Chem.*, 2006,
449 **118**, 5066.
- 450 15 Y. Sato, T. Iwata, S. Tokutomi and H. Kandori, *J. Am. Chem. Soc.*, 2005, **127**, 1088.
- 451 16 Y. Zhou and J. Yoon, *Chem. Soc. Rev.*, 2012, **41**, 52.
- 452 17 X. Chen, T. Pradhan, F. Wang, J. S. Kim and J. Yoon, *Chem. Rev.*, 2012, **112**, 1910.
- 453 18 X. Yang, Y. Guo and R. M. Strongin, *Angew. Chem. Int. Ed.*, 2011, **50**, 10690.
- 454 19 L. He, B. Dong, Y. Liu and W. Lin, *Chem. Soc. Rev.*, 2016, **45**, 6449.
- 455 20 L. Y. Niu, Y. Z. Chen, H. R. Zheng, L. Z. Wu, C. H. Tung and Q. Z. Yang, *Chem. Soc. Rev.*,
456 2015, **44**, 6143.
- 457 21 Z. L. Lu, Y. N. Lu, C. H. Fan, X. Sun, W. Q. Shao, N. Jiang, X. Y. Gong, Y. Z. Lu, G. X.
458 Sun and X. C. Jiang, *Sens. Actuators B*, 2019, **290**, 581.
- 459 22 D. J. Zhu, X. W. Yan, A. S. Ren, W. Xie and Z. H. Duan, *Anal. Chim. Acta*, 2019, **1058**,
460 136.
- 461 23 P. Srivastava, R. C. Gupta and A. Misra, *ChemistrySelect*, 2018, **3**, 12900.
- 462 24 J. Li, Y. k. Yue, F. J. Huo and C. X. Yin, *Dyes Pigments*, 2019, **164**, 339.
- 463 25 W. Zhang, X. Y. Zhao, W. J. Gu, T. Cheng, B. X. Wang, Y. L. Jiang and J. Shen, *New J.*
464 *Chem.*, 2018, **42**, 18109.

- 465 26 S. Jiao, X. He, L.B. Xu, P.Y. Ma, C. M. Liu, Y. B. Huang, Y. Sun, X. H. Wang and D. Q.
466 Song, *Sens. Actuators B*, 2019, **290**, 47.
- 467 27 Z. L. Lu , Y. N. Lu , C. H. Fan , X. Sun , W.Q. Shao, N. Jiang , X. Y. Gong , Y. Z. Lu , G.
468 X. Sun and X. C. Jiang, *Sens. Actuators B*, 2109, **290**, 581.
- 469 28 D. G. Chen, Z. Long, Y. C. Dang and L. Chen, *Dyes Pigments*, 2019, **166**, 266.
- 470 29 K. S Lee, T. K Kim, J. H. Lee, H. J. Kim and J. I. Hong, *Chem. Commun.*, 2008, **46**, 6173.
- 471 30 Z. G. Yang, N. Zhao, Y. M. Sun, F. Miao, Y. Liu, X. Liu, Y. H. Zhang, W. T. Ai, G. F.
472 Song, X. Y. Shen, X. Q. Yu, J. Z. Sun and W. Y. Wong, *Chem. Commun.*, 2012, **48**, 3442.
- 473 31 M. J. Wei, P. Yin, Y. M. Shen, L. L. Zhang, J. H. Deng, S. Y. Xue, H.T. Li, B. Guo, Y. Y.
474 Zhang and S. Z. Yao, *Chem. Commun.*, 2013, **49**, 4640.
- 475 32 W. S. Qua, L. Yang, Y. D. Hang, X. Zhang, Y. Qu and J. L. Hua, *Sens. Actuators B*, 2015,
476 **211**, 275.
- 477 33 X. F. Hou, Z. S. Li, B. L. Li, C. H. Liu and Z. H. Xu, *Sens. Actuators B*, 2018, **260**, 295.
- 478 34 Y. Tian, B. C. Zhu, W. Yang, J. Jing and X. L. Zhang, *Sens. Actuators B*, 2018, **262**, 345.
- 479 35 H. Fang, N. Wang, L. Xie, P.C. Huang, K. Y. Deng and F. Y. Wu, *Sens. Actuators B*, 2019,
480 **294**, 69.
- 481 36 L. H. Liu, Q. Zhang, J. Wang, L. L. Zhao, L. X. Liu and Y. Lu, *Talanta*, 2019, **198**, 128.

- 37 X. Y. He, X. F. Wu, W. S. and H. M. Ma, *Chem. Commun.*, 2016, **52**, 9410.
- 38 H. J. Xiang, H. P. Tham, M. D. Nguyen, S. Z. F. Phua, W. Q. Lim, J. G. Liu and Y. L. Zhao, *Chem. Commun.*, 2017, **53**, 5220.
- 39 L. H. Zhai, Z. L. Shi, Y. Y. Tu and S. Z. Pu, *Dyes Pigments*, 2019, **165**, 164.
- 40 J. Li, Y. Yue, F. Huo and C. Yin, *Dyes Pigments*, 2019, **164**, 335.
- 41 B. Dong, Y. Lu, N. Zhang, W. Song and W. Zhang, *Anal. Chem.*, 2019, **91**, 5513.
- 42 D. Zhu, X. Yan, A. Ren, W. Xie and Z. Duan, *Anal. Chim. Acta*, 2019, **1058**, 136.
- 43 X. Li, H. Ma, J. Qian, T. Cao, Z. Teng, K. Iqbal, W. Qin and H. Guo, *Talanta*, 2019, **194**, 717.
- 44 W. Xuan, Y. Cao, J. Zhou and W. Wang, *Chem. Commun.*, 2013, **18**, 10474.
- 45 K. Huang, M. Liu, Z. Liu, D. Cao, J. Hou and W. Zeng, *Dyes Pigments*, 2015, **118**, 88.
- 46 L. He, X. Yang, K. Xu and W. Lin, *Anal. Chem.*, 2017, **89**, 9567.
- 47 S. Yang, C. Guo, Y. Li, J. Guo, J. Guo, J. Xiao, Z. Qing, J. Li and R. Yang, *ACS Sens.*, 2018, **3**, 2415,
- 48 J. Zhang, X. Y. Zhu, X. X. Hu, H. W. Liu, J. Li, L. L. Feng, X. Yin, X. B. Zhang and W. H. Tan, *Anal. Chem.*, 2016, **88**, 11892.
- 49 K. Huang, L. Yu, P. Xu, X. Zhang and W. Zeng, *RSC Adv.*, 2015, **5**, 17797.
- 50 X. Zhu, M. Xiong, H. Liu, G. Mao, L. Zhou, J. Zhang, X. Hu, X. B. Zhang and W. Tan, *Chem. Commun.*, 2016, **52**, 733.

501 51 J. Li, Y. Yue, F. Huo and C. Yin, *Dyes Pigments*, 2019, **164**, 335.

502 52 B. Dong, Y. Lu, N. Zhang, W. Song and W. Lin, *Anal. Chem.* 2019, **91**, 5513.

503 53 L. Fan, W. Zhang, X. Wang, W. Dong, Y. Tong, C. Dong and S. Shuang, *Analyst*, 2019,

504 **144**, 439.